Analytical and Experimental Investigation for the Effect of Air Injection Angle on the Performance of Airlift Pump

Ali Abdul Mohsin Hasan Alasadi
Assistant Professor
College of Engineering-University of Baghdad
dralicit @yahoo.com

Ahmed Khalid Habeeb
M.Sc.
College of Engineering-University of Baghdad
eng_ahmedkhalid@yahoo.com

ABSTRACT

The effect of air injection angle on the performance of airlift pump used for water pumping has been studied analytically and experimentally. An airlift pump of dimensions 42mm diameter and 2200 mm length with conventional and modified air injection device was considered. A modification on conventional injection device (normal air-jacket type) was carried out by changing injection angle from 90° (for conventional) to 45° and 22.5° (for modified). Continuity and one-dimensional momentum balance for the flow field with basic principle of two-phase flow and expressions of slip ratio and friction factor as function of flow rates were formulated. The analytical and experimental investigations were carried out for both conventional and unconventional air-jackets at submergence ratios 0.75, 0.6 and 0.5 and air mass flow rate from 0.5 to 97kg/hr. The comparison between the analytical and experimental results shows agreement and the main results showed that the performance and maximum efficiency of airlift pump is increased for higher mass flow rate of injected air for all tested submergence ratio using unconventional air-jacket and the higher performance was associated with injection angle 22.5°, with average enhancement were 9% and 10% for performance and maximum efficiency respectively.

Key words: airlift pump, air injection angle, submergence ratio, two-phase flow

دراسة تحليلية وعملية حول تأثير زاوية حقن الهواء على أداء مضخات الرفع الهوائية

علي عبد المحسن حسن الاسدي
أستاذ مساعد
كلية الهندسة-جامعة بغداد

احمد خالد حبيب
ماجستير
كلية الهندسة-جامعة بغداد

الخلاصة

تم إجراء دراسة تحليلية وعملية حول تأثير زاوية حقن الهواء على أداء مضخات الرفع الهوائية التي تستخدم في رفع الماء. تم الأخذ بنظر الاعتبار مضخة رفع هوائية بقطر 42 ملم لأنبوب الرفع وبطول 2200 ملم باستخدام منظومة حقن هواء تقليدية ومنظومة أخرى معدلة. تم تعديل منظومة حقن الهواء التقليدية نوع (Air-Jacket) من خلال تغير زاوية الحقن من 90 درجة (للمنظومة التقليدية) إلى زاوية 45 و 22.5 درجة (للمنظومة المعدلة). تم في الدراسة التحليلية بناء موديل رياضي اعتمادا على قانون حفظ الكتلة وقانون الزخم أحادي البعد لمنطقة الجريان واستخدام المبادئ الأساسية لجريان ثنائي الأطوار بالإضافة إلى المعادلات الخاصة بنسبة الانزلاق ومعامل الاحتكاك وتم إجراء الحل الرياضي والفحص العملي للمضخة مع منظومة حقن تقليدية ومعدلة عند نسبة غمر مقدارها 0.75، 0.6، 0.5 مع معدل تدفق كتلة الهواء المحقون من 0.5 إلى 97 كغم/ساعة. بينت المقارنة

بين النتائج التحليلية والنتائج العملية مقبولية جيدة قد أظهرت النتائج زيادة في أداء وكفاءة المضخة عند معدلات الحقن العالية عند استخدام منظومة الحقن المعدلة لكل ظروف الفحص، وان أفضل زاوية حقن هي 22.5 درجة مع تحسن 9% في الأداء و 10% لأعلى كفاءة.

الكلمات الرئيسية: مضخات الرفع الهوائية، زاوية حقن للهواء، نسبة الغمر، جريان ثنائي الطور.

1. INTRODUCTION

Airlift pump is generally regarded to be part of a unique kind of alternative pumping technology. The importance of this technology is arising when rotodynamic pumps are inappropriate for a given application. Most of these application that uses the technologies involve mixture of fluid-solid, very viscous fluid, hazardous fluids, fluid containing live organisms suspend in fluid, situation of low head or low submergences, applications with variable inlet water surface level and irregular shape wells. This class of pumps has simplicity in design and absence of moving and rotating parts which made the maintenance easy with low cost and high reliability. From the very beginning of the 20th century and in order to predict the airlift pump performance many analytical studies have been developed. **Stenning and Martin, 1968,** developed analytical model using one-dimensional continuity and momentum equations together with the basic relation of two-phase flow. A comparison with experimental work is carried out, and they predicted that the theory of one-dimensional flow gives a good knowledge for the analysis of airlift pump performance and they recommended using the model for pumps working in larger depths by dividing the pipe length into segments for which the density of air can be considered constant. This model is extended by, **Parker, 1980,** in order to take into consideration the momentum of injected air when nozzle injection device is used. He found that size and number of injection holes of air-jacket does not affect the discharge characteristic of the pump, and the nozzle design gives higher pumping rate at high air mass flow rates for small orifice area, but with very low efficiency. **Chisholm, 1982,** developed simple expressions based on homogenous theory to predict rapidly the performance, fraction of mass dryness and total mass flow rate of airlift pumps at "Maximum Flow Condition". The predicted mass flow rate is compared with theoretical and experimental of, **Stenning and Martin, 1968,** and found to be within 15%. **Clark and Dabolt, 1986,** developed a general design equation for airlift pumps working in slug flow pattern by extending the theory of, **Nicklin, 1963,** to long pumps. An explicit formula of design equation is obtained by integrating the combination of momentum, friction loss and void fraction expression over the complete length of the pump. The new design equation is supported experimentally using variety of liquids and submergence ratios. They stated that design of airlift pump using this method is more rapid with less energy required than the incremental procedure, as well as the method is more accurate than the results of existing empirical equation. **Reinemann et al., 1990,** extended the theory proposed previously by, **Nicklin, 1963,** into small diameter airlift pump from 3 mm to 25 mm by taking into consideration the effect of surface tension on the gas void rising velocity. They noted a difference between the rise velocity of single gas slug and train of gas slugs in small vertical tube. They noted that the efficiency increased for this range of tube diameter. **De Cachard and Delhaye, 1996,** proposed a new steady state model to predict the performance of small airlift pump (less than 40 mm) by combination of specific model describing slug and churn flow and supported his work by experimental investigation. They reported that the new proposed model is more accurate tool than the existing model in design small airlift pump with diameter up to 40 mm and length to diameter ratio greater than 250. **Kassab et al., 2009,** developed a modified version of the model proposed by, **Stenning and Martin, 1968,** by introducing slip ratio as expressed by, **Griffith and Wallis, 1961,** for slug flow and the friction factor which is obtained from Colebrook equation, **Haaland, 1983**. The

proposed modified model is compared with the experimental results that predicted by, **Kassab et al., 2001,** as well as, the theoretical prediction using the proposed model of, **Stenning and Martin, 1968,** and, **Clark and Dabolt, 1986.** They reported that the model of **Clark and Dablot** is appropriate only for the first zone of pump performance curve where the flow pattern is slug and the modified one-dimensional model gives more agreement with the experimental results for airlift pump working in different flow pattern (bubbly, slug and churn) except the annular flow.

The present work investigates analytically and experimentally the effects of changing the injection angle of injection device (air-jacket) at various submergence ratios and mass flow rate of injected air on the performance of airlift pump. A regular airlift pump with conventional and modified air-jacket is considered in this work.

2. EXPERIMENTAL WORK

The experimental work has been carried out in the Fluid Mechanics Laboratory in the Department of Mechanical Engineering - Collage of engineering/University of Baghdad in order to obtain water discharge rate and analyze the structure of flow filed within riser pipe. The experimental setup is shown in **Fig.1 and Fig.2** and the equipment used in the experimental work consists of:

2.1 Test Rig

The test rig consists of the riser pipe which is a transparence smooth pipe made of acrylic resin with 2000 mm length and 42mm inner diameter. The discharge side (upper end) of the riser pipe is connected to a collecting header of 4" diameter made of PVC. The highest point of the header is opened to ambient which allows air to escape from the pumped mixture. The lower end of the collecting header is divided into two branches with 2" PVC quick closing ball valve at its end to direct water from riser either, to intermediate tank or to metering tank. A 0.5 hp electric centrifugal water pump has maximum head of 35 m and maximum discharge of 36 litters/minute is used to pump water from the intermediate tank to the movable tank. The movable tank is a cylindrical tank holed by steel cable connected to a manual hoist can be moved upward and downward in order to change the submergence ratio and feed the riser pipe with water at constant head through the transient tank. A 1" quick closing ball valve made of brass is fitted at the bottom side of the transient tank as inlet to the tank. The riser pipe is fitted to the transient tank through the injection device, in which the compressed air is distributed uniformly and injected into the riser pipe to perform the pumping action. The injection device is designed as three independent injection stages, each stage delivered air through two ports and have 52 holes per stage drilled of diameter 3mm distributed in two rows and holes center line are inclined from injector wall by $90^{\circ}, 45^{\circ}, 22.5^{\circ}$ for the first, second and third stages respectively. Injection device with holes center line vertical to the injector wall (90°) is considered as normal or standard air jacket. All the elements above of the test rig are assembled to gather in a main steel frame. The frame is made of standard 2" galvanized angle iron rack, fabricated into proper length and connected to gather.

2.2 Air Supply System

The experimental work is performed using a high pressure air compressor which delivered 1.05 m^3/min with a storage vessel of 1200 lit capacity and cutoff pressure of 14 bar, this compressor supply compressed air to a pressure reducing valve (0.5 – 5) bar to ensure a constant air pressure supply from the compressor. A constant area air flow meter of range (2 – 27) m^3/hr is used to

measure the volume flow rate of injected air and the temperature of supplied air was measured by a calibrated thermocouple. A needle valve 3/4" made of stainless steel is used to control the volume flow rate of injected air to the rig, as well as a 3/4" quick closing ball valve made of brass is used to simultaneously cutoff air supplying to the rig.

2.3 Experimental Procedure

The main part of the experiment was the measuring of the water discharged from the airlift pump for different angles of injection. The experimental procedures are as follows:

1. The air compressor is started and the pressure reducing valve is adjusted to the desired pressure.
2. The connection hose of the air system is linked to the desired stage of injection.
3. The centrifugal pump is started.
4. The level of movable tank is adjusted to the desired submergence ratio.
5. Injection of compressed air into the pipe is started; the needle valve is adjusted to the desired volume flow rate(Q_{air}), then the pressures(P_{air}) and temperature(T_{air}) are recorded.
6. The air mass flow rate is computed from the following equation:

$$\dot{m}_{air} = \rho_{air} \times Q_{air} \quad (1)$$

Where the density of air is calculated using ideal gas equation:

$$\rho_{air} = \frac{P_{air}}{R \times T_{air}} \quad (2)$$

7. The system is left to reach quasi- steady state.
8. The discharged water from intermediate tank is directed to the metering tank for a certain time (usually is taken 20 s) by closing the valve at the end of the collecting header which routed the water to the intermediate tank and open the other to the metering tank:
9. The volume of water accumulated in the metering tank ($V_{accumilate}$) is recorded.
10. The water mass flow rate is computed from the following equation:

$$\dot{m}_{water} = \rho_{water} \times \frac{V_{accumilate}}{t} \quad (3)$$

11. An estimation of flow regime type is reported.
12. The ball valves 14 and 15 are simultaneously closed, **Hamid et al., 2013**:
13. The retained volume of the riser (V_L) is recorded and the volumetric void fraction is computed from the equation:

$$\alpha = 1 - \frac{V_L}{\text{total volume of riser}} \quad (4)$$

(7) and (8) are repeated three times for each mass flow rate of air and take the average results.

The procedure above is repeated for different submergence ratio and injection angle for the same range of air mass flow rate.

A high speed camera made by SAMSUNG (model WB2000, 10 megapixels and 1000 f/s) is used to capture photos of flow regime detected in the riser tube, and water is colored by adding a light color in order to make the reorganization of flow pattern easier.

2.4 Error Analysis

Deviation was calculated for the experimental data using the formula for calculating percentage error as:

$$\text{Percentage error} = \left(\frac{\text{measured value} - \text{estimated value}}{\text{measured value}}\right) * 100 \quad (5)$$

Where measured values are result from the experimental work and the estimated value from the theoretical.

3. MATHMATICAL FORMULATION

The basic model that was proposed by, **Stenning and Martain, 1968,** based on assumption of steady state one-dimensional flow in the pump riser, continuity and momentum equations together with the basics principles of two phase flow is used to solve the governing equations analytically. The modification is carried out to take account of the effect of momentum due to the velocity component of air injected in flow direction as well as, the characteristic of flow pattern that occurred at best operation of air lift pump was considered, **Kassab et al., 2009**. However, because of the steady state one-dimensional nature of these analytical models, they are inadequate of providing vision and information about the characteristic of different flow patterns developed in the riser pipe of the pump and the transient nature of the pumping process, **Wahba et al., 2014**.

3.1Governing Equations

In the present work, the working fluids are water and air and the following assumptions are made:

1. Planes of equal velocity and equal pressure are normal to the pipe axis which is makes the case one-dimensional).
2. No exchange of mass between phases.
3. Isothermal flow for all phases.
4. Incompressible for the air phase.
5. Newtonian fluids.
6. Constant properties of air and water.
7. Neglect the pressure of compressed air at inlet.

Consider the airlift pump basically is a vertical pipe with a diameter D and total length L, partially full of water with reference height (zero) at the base of the pipe, the pump is divided into two parts, injection zone and the remained of the riser as shown in **Fig.3** Governing equations are applied to each part and the results combined together to obtain a non-linear equation governing the complete pump, **Stenning and Martain, 1968**. The governing equations basically are:

Continuity equation:

$$\sum \rho \vec{u} A = 0 \tag{6}$$

Momentum equation:

$$\sum \rho u A \vec{u} = \sum F \tag{7}$$

3.1.1 Injection Zone

The pump is partially immersed in water (surrounding field) into a height of Hs, Bernoulli's equation is applied between free surface of water and the pump inlet (1) in order to take in account the effect of the static head of immersed length as follow:

$$P_1 = P_a + \rho_L g H_s - \frac{1}{2}\rho_L u_1^2 \quad (8)$$

where: u_1 is the velocity of water at the inlet to the pump.

To find a relation for the velocity and density leaving the injection zone with the velocities and densities entered to the zone, the continuity equation is applied for the control volume between (1) and (2) as shown in **Fig.3**, neglecting the changes of air density, **Kassab et al. 2009**, is written as:

$$Au_2 = Q_g + Q_L \quad (9)$$

where u_2 is the velocity of mixture (water and air) leaving the injection zone, and $Q_L = Au_1$ is the water flow rate inlet to the pump.

Divided Eq. (9) by Q_L which is yield:

$$u_2 = u_1\left(1 + \frac{Q_g}{Q_L}\right) \quad (10)$$

The air mass flow rate entered to the injection zone is too small if compared with the water mass flow rate, therefore the air mass flow rate can be neglected and the continuity equation can be written again as:

$$\rho_2 A u_2 = \rho_L A u_1 \quad (11)$$

and rearranging

$$\rho_2 = \rho_L \frac{u_1}{u_2} \quad (12)$$

By substituting Eq. (10) in to Eq. (12) yields mixture density as function of inlet air flow rate, inlet water flow rate and water density as shown:

$$\rho_2 = \frac{\rho_L}{\left(1 + \frac{Q_g}{Q_L}\right)} \quad (13)$$

The momentum equation is applied for the control volume between (1) and (2), neglecting the friction losses of wall, **Parker, 1980**, and is written as:

$$AP_1 - AP_2 = \left(\rho_L Q_L + \rho_g Q_g\right)u_2 - \rho_L Q_L u_1 - \rho_g Q_g u_g cos\theta \quad (14)$$

where $u_g\cos\theta$ is the vertical component of injected air velocity in the direction of main flow.

Since $\rho_g Q_g <<< \rho_L Q_L$ therefore the term $\left(\rho_L Q_L + \rho_g Q_g\right)$ on the right hand side of Eq. (14) is approximately $\approx \rho_L Q_L$ and Eq. (14) reduces to:

$$AP_1 - AP_2 = \rho_L Q_L u_2 - \rho_L Q_L u_1 - \rho_g Q_g u_g cos\theta \quad (15)$$

Substituting Eq. (10) into Eq. (15) and rearrange, the result equation becomes:

$$P_2 = P_1 - \rho_L \frac{Q_g}{A} u_1 + \rho_g \frac{Q_g}{A} u_g cos\theta \quad (16)$$

The total air flow rate injected in the pump Q_g is equal to the summation of air flow rate of each injection hole of injection device, as:

$$Q_g = \sum Q_{hole} \quad (17)$$

The design of injection device is ensured evenly distribution of injection air on the all holes, therefore, Eq. (17) becomes:

$$Q_g = u_g N A_{hole} \quad (18)$$

and

$$A_j = N A_{hole} \quad (19)$$

where A_j is the total area of injection holes, N is number of holes and A_{hole} is the area of a hole. Combining Eqs. (8), (18), (19) and (16) gives the pressure at the outlet of injection zone depending on the parameters of the zone, as follows:

$$P_2 = P_a + \rho_L g H_s - \frac{1}{2}\rho_L u_1^2 - \rho_L \frac{Q_g}{Q_L} u_1^2 + \rho_L u_1^2 \frac{\rho_g}{\rho_L}\frac{A}{A_j}\left(\frac{Q_g}{Q_L}\right)^2 cos\,\theta \quad (20)$$

3.1.2 The Riser Pipe

The momentum equation is applied for the control volume between (2) and discharges of the pipe, **Fig.3**, and taking into consideration the friction losses of wall and the weight of the mixture in the pipe as follows:

$$P_2 = P_a + \frac{\tau_w \pi D L}{A} + \frac{W}{A} \quad (21)$$

where τ_w is the average shear stress for slug flow of riser wall and is suggested by, **Griffth and Wallis, 1961,** and, **Kassab et al., 2009,** and W is the weight of mixture in the riser pipe, **Parker, 1980,** as follows:

$$\tau_w = f\frac{\rho_L}{2}\left(1 + \frac{Q_g}{Q_L}\right)\left(\frac{Q_L}{A}\right)^2 \quad (22)$$

$$W = \frac{\rho_L g L A}{\left(1 + \frac{Q_g}{S Q_L}\right)} \quad (23)$$

where f is the friction factor of the wall assuming water alone flows through the riser with flow rate equal to $(Q_L + Q_g)$ and is obtained using Colebrook formula, **Haaland, 1983,** as:

$$\frac{1}{\sqrt{f}} = -2.0\,log\left(\frac{\epsilon/D}{3.7} + \frac{2.51}{Re\sqrt{f}}\right) \quad (24)$$

and S is slip ratio and equals to:

$$S = \frac{u_{ga}}{u_{La}} \quad (25)$$

where u_{ga} and u_{La} are phase actual velocities of air and water respectively in the riser pipe**, Kreith et al., 1999**.

Substituting Eq. (22) and (23) into Eq. (21) gives a correlation of P_2 (pressure at the outlet of injection zone) in terms of the parameters of the riser pipe, as follows:

$$P_2 = P_a + K\left(\frac{\rho_L u_1^2}{2}\right)\left(1 + \frac{Q_g}{Q_L}\right) + \frac{\rho_L g L}{\left(1 + \frac{Q_g}{S Q_L}\right)} \quad (26)$$

3.1.3 The Complete Pump

The performance equation for the whole pump is determined by equating Eq. (20) and Eq. (26) and rearranging gives:

$$\frac{H}{L} - \frac{1}{\left(1 + \frac{Q_g}{S Q_L}\right)} = \frac{Q_L^2}{2gLA^2}\left[(K+1) + (K+2)\frac{Q_g}{Q_L} - 2\frac{\rho_g}{\rho_L}\frac{A}{A_j}\left(\frac{Q_g}{Q_L}\right)^2 cos\theta\right] \quad (27)$$

where S is described as a function of water and air flow rate by, **Griffth and Wallis, 1961,** and, **Kassab et al., 2009,** for slug flow as:

$$S = 1.2 + 0.2\frac{Q_g}{Q_L} + \frac{0.35\sqrt{gD}}{V_1} \quad (28)$$

and

$$K = \frac{4fL}{D} \quad (29)$$

All other losses due to water entrance losses, sudden expansion, elbow, tee and valves are accounted by increasing the effective value of K.

The term $\left[2\frac{\rho_g}{\rho_L}\frac{A}{A_j}\left(\frac{Q_g}{Q_L}\right)^2 cos\theta\right]$ in the right hand side of the non-liner Eq. (27) , is considered a gain of air momentum that affected the performance in the direction of main flow and the angle θ governed this effect, therefore, for $\theta = 90$ the term is disappeared from the equation and reduced to the same equation derived by, **Stenning and Martin, 1968,** for standard air-jacket injection device, and vice versa, for $\theta = 0$, yield the same performance equation for air-nozzle injection device derived by, **Parker, 1980**, therefore Eq. (27) is theoretically applicable to find the performance of airlift pumps range from standard air-jacket to air-nozzle device and between them for various injection angle.

3.2 Method of Solution

The theoretical performance of airlift pump was evaluated by solving the governing equation (Eq. (27)) by iteration and a corresponding computer program is developed for this purpose. Solution procedure is described in steps as follows:

1. The geometrical parameters $D, L, \epsilon, d_j, N, and\ \theta$ is introduced and sub calculations to find A and $A_j$are performed.
2. H_s is introduced corresponding with selected submergence ratio as follows:
   $$\mathrm{Sr} = \frac{\mathrm{H}}{\mathrm{L}} \quad (30)$$
3. Properties for water and air for certain condition are assigned.
4. Inlet air flow rate is assigned.
5. A trial value for water flow rate is assumed.
6. Reynolds number is calculated assuming water alone flows through the riser with flow rate equal to $(Q_L + Q_g)$
7. Friction coefficient f is calculated from Colebrook Eq. (24) by trial and error, and then K is calculated from Eq. (29).
8. Slip ratio from Eq. (28) is calculated.
9. New value (better approximation) of water flow rate ($\mathrm{newQ_L}$) is calculated by solving equation (27) using proper iterative method.
10. The procedure from step 5 is repeated with new trial value of water flow rate until the total absolute difference between $\mathrm{newQ_L}$ and assumed $\mathrm{Q_L}$becomes less than 10^{-6}.

Newton-Raphson method is used to solving the set of the equations, **Alan, 2002,** and a computer program is built for implementing the solution procedure by employing MATLAB R2013b software.

3.3 Airlift Pump Characteristics

The most important airlift pump characteristics in this work are the water pumping rate, and efficiency coefficients. Application of continuity and momentum conservation laws give amount of pumped water for specified operational and geometrical parameters. Once water flow rate is predicted, other pump characteristics can be found directly. Efficiency (η) of airlift pump is defined by, **Nicklin, 1963,** as a ratio of beneficial work done in water to the energy released from the isothermal expansion of injected air from injection pressure to the ambient pressure as follows:

$$\eta = \frac{g\rho_L Q_L (L - H_s)}{P_a Q_g \ln(P_{in}/P_a)} \quad (31)$$

4. RESULTS

In general, performance curve of any airlift pump shows the behavior of the pump output over the input range of air; it is obtained by plotting the values of induced water mass flow rate against input air mass flow rate at a specified value of submergence ratio and injection angle. **Fig.4** shows performance curve predicted using the proposed analytical model as well as the results of experimental work. As expected, injection device with angles (45° and 22.5°) gives higher water mass flow rate at higher mass flow rates of injected air than the conventional air-jacket with injection angle (90°) for all tested submergence ratios, this increasing of water flow rate can be related to the initial momentum result from the velocity component of injected air in the flow direction in the riser pipe. A comparison of performance curve between the experimental and analytical prediction for the same investigation conditions are in agreement with average deviation about 9%, 17% and 23% for submergence ratios of 0.5, 0.6 and 0.75 respectively.

Fig.5 shows the variation of analytical and experimental performance curves with submergence ratio, these curves for each injection angle at different submergence ratios have similar trend and shows that decreasing in pumped water mass flow rate is associated with decreasing in submergence ratio, this is true, because when submergence ratio decreases, the length that the water should traverse is increased through the riser pipe and this length is proportional to the lifting head ($L - H_s$). The average enhancement results from modifying conventional air-jacket by changing the injection angle from (90°) to (45° and 22.5°) based on experimental results are, increasing the pumping rate about 8% for injection angle (45°) and 11% for injection angle (22.5°), while the average enhancement based on the analytical results are 10% for injection angle (45°) and 14% for injection angle (22.5°).

The variation of efficiency of the airlift pump, which is obtained from proposed model and experimental work, with injection angle at a specified submergence ratio are shown in **Fig.6**. Both, analytical and experimental efficiency results has similar trend that the efficiency increased rapidly from its minimum value (0) until a maximum value is achieved then decreases gradually. It was noticed that the maximum efficiency increased for injection angle 45° and 22.5°, and this increase is related to the increasing of work done by the pump which is associated with increasing of water output from the pump for the same mass flow rate of injected air and submergence ratio. The comparison between predicted efficiencies from the proposed model and experimental efficiency for the same investigation conditions shows good agreement with average deviation of 8%, 12% and 9% for submergence ratio 0.5, 0.6 and 0.75 respectively. The increase in maximum efficiency based on the experimental results is about 9% for injection angle 45° and 11% injection angle 22.5°.

To discuss the behavior of air lift pump efficiency with the water flow rate at a specified injection angle and submergence ratio, efficiency curve and performance curve are plotted together in one figure as shown in **Fig.7**, it is observed for all investigated cases that the maximum efficiency achieved by airlift pump dose not correspond to the maximum output water mass flow rate due to the transition of flow pattern from stable slug flow to churn flow which is characterized as chaotic and unstable. Another observation that the best efficiency points achieved when the flow is slug and slug-churn flow, this is approved by comparing the distribution of best experimental efficiencies on the flow map proposed by, **Taitel et al., 1980**, and **Fig.8, Fig.9 and Fig.10** shows that the best efficiency points located at slug and slug-churn zones.

5. CONCLUSIONS

- The optimum angle of air injection was found to be at 22.5° for the selected operational and geometrical parameters.
- Average enhancement of airlift pump performance is about 8% for air injection angle 45° and 11% for 22.5°.
- Increasing of water mass flow rate as the submergence ratio increased for all tested injection angle and the maximum mass flow rate of water achieved is 2794, 2371 and 1720 kg/hr for submergence ratio 0.75, 0.6 and 0.5 respectively.
- Maximum efficiency is increased as the submergence ratio increased and maximum efficiency achieved is 36%, 32% and 30% for submergence ratio 0.75, 0.6 and 0.5 respectively.
- Maximum efficiency of airlift pump does not occur with the maximum mass flow rate of water.
- Best efficiency points corresponds to the slug and slug-churn flow pattern, therefore, it's recommended to operate any airlift pump with these patterns of flow.
- The proposed one-dimensional analytical model is incapable of providing any information about the flow patterns and transient nature of the flow.
- The proposed one-dimensional analytical model gave better results and good agreement with experimental results and the proposed analytical model can be used as efficient tool in predicting the overall performance and design of airlift pump.

NOMENCLATURE

A = cross section area of the riser pipe, m^2
A_{hole}= area of injection hole, m^2
A_j= total areas of injection, m^2
D= diameter of riser pipe, m
D_h= hydraulic diameter, m
D= diameter of injection hole, m
F= force, N
f= friction factor
g= gravity acceleration, m/s^2
H_s = static Head or Submerged length, m
K = friction parameter
L = length of riser pipe, m
$\dot{m}$= mass flow rate, kg/s

N= number of holes
P= pressure, N/m^2
Q= volume flow rate, m^3/s
Q_{hole}= air volume flow rate per hole, m^3/s
Re = Reynolds number
S = slip ratio
u= velocity, m/s
$\bar{u}$= velocity vector, m/s
V= volume, m^3
W= weight of mixture in the riser pipe, N
θ= angle of air injection, Degree
ϵ= pipe roughness, m
μ= molecular or dynamic viscosity, kg/m.s
P= density, kg/m^3
τ_w= wall shear stress, N/m^2
η= efficiency

SUBSCRIBIES

g= gas
L= liquid
ga= gas average
La=liquid average
gs= gas superficial
Ls= liquid superficial
a= ambient

REFRENCES

- Alan Jeffrery, 2002, *Advance Engineering Mathematics*, Harcourt/Academic press.
- Chisholm D., 1982, *Prediction of the performance of air-lift pumps*, International Journals of Heat and Fluid Flow, Vol. 3, pp. 149-152.
- Clark, N.N., Dabolt, R.J., 1986, *A general design equation for air-lift pumps operating in slug flow*, AICHE J., Vol. 32, pp. 56–64.
- De Cachard F., Delhaye J.M., 1996, *A slug-churn model for small- diameter airlift pumps*, Int. J. Multiphase Flow, Vol. 22, pp. 627-649.
- Griffith, P., Wallis, G.B., 1961, *Two-phase slug flow*, J. Heat Transfer, Trans. ASME, Vol. 83, pp. 307–320.
- Haaland S. E., 1983, *Simple and Explicit Formulas for the Friction Factor in Turbulent Pipe Flow*, Journal of Fluids Engineering, , Vol. 105, pp. 89-90.
- Kassab, S.Z., Kandil, H.A., Warda, H.A., Ahmed, W.H., 2001, *Performance of an air lift pump operating in two-phase flow*, in Proceedings of ICFDP7: The Seventh International Congress on Fluid Dynamics & Propulsion, Cairo, Egypt, Paper No. ICFDP7-2001004.
- Kassab Sadek Z., Hamdy A. Kandil, Hassan A. Warda, Wael H. Ahmed, 2009, *Air-lift pumps characteristics under two-phase flow conditions*, International Journal of Heat and Fluid Flow, Vol.30, pp. 88–98.

- Kreith Frank, Berger A., Churchill W., Tullis P., White M., 1999, *Fluid Mechanics*, Mechanical Engineering Handbook, CRC press LLC.
- Nicklin D. J., 1963, *The airlift pump theory and optimization*, International chemical Eng., Vol. 41, pp. 29-39.
- Parker G. J., 1980, *The Effect of Footpiece Design on the Performance of a Small Air Lift Pump*, INT. J. HEAT & FLUID FLOW, Vol. 2, No. 4, pp. 245-252.
- Reinemann D. J., J. Y. Parlange, M. B. Timmons, 1990, *Theory of Small-Diameter Airlift Pump*, I. J. Multiphase flow, Vol. 16, pp. 113-122.
- Stenning, A.H., Martin, C.B., 1968, *An analytical and experimental study of air lift pump performance*, J. Eng. Power, Trans. ASME' Vol. 90, pp.106–110.
- Taitel Yehuda, Dvora Bornea, A. E. Dukler, 1980, *Modeling Flow Pattern Transitions for Steady Upward Gas-Liquid Flow in Vertical tubes*, AICh journal, Vol. 26, No. 3, pp. 345-354.
- Wahba E. M., M. A. Gadalla, D. Abueidda, A. Dalaq, H. Hafiz, K. Elawadi and R. Issa, 2014, *On the Performance of Air-Lift Pumps: From Analytical Models to Large Eddy Simulation*, Journal of Fluids Engineering, Vol. 136, pp.1-7.

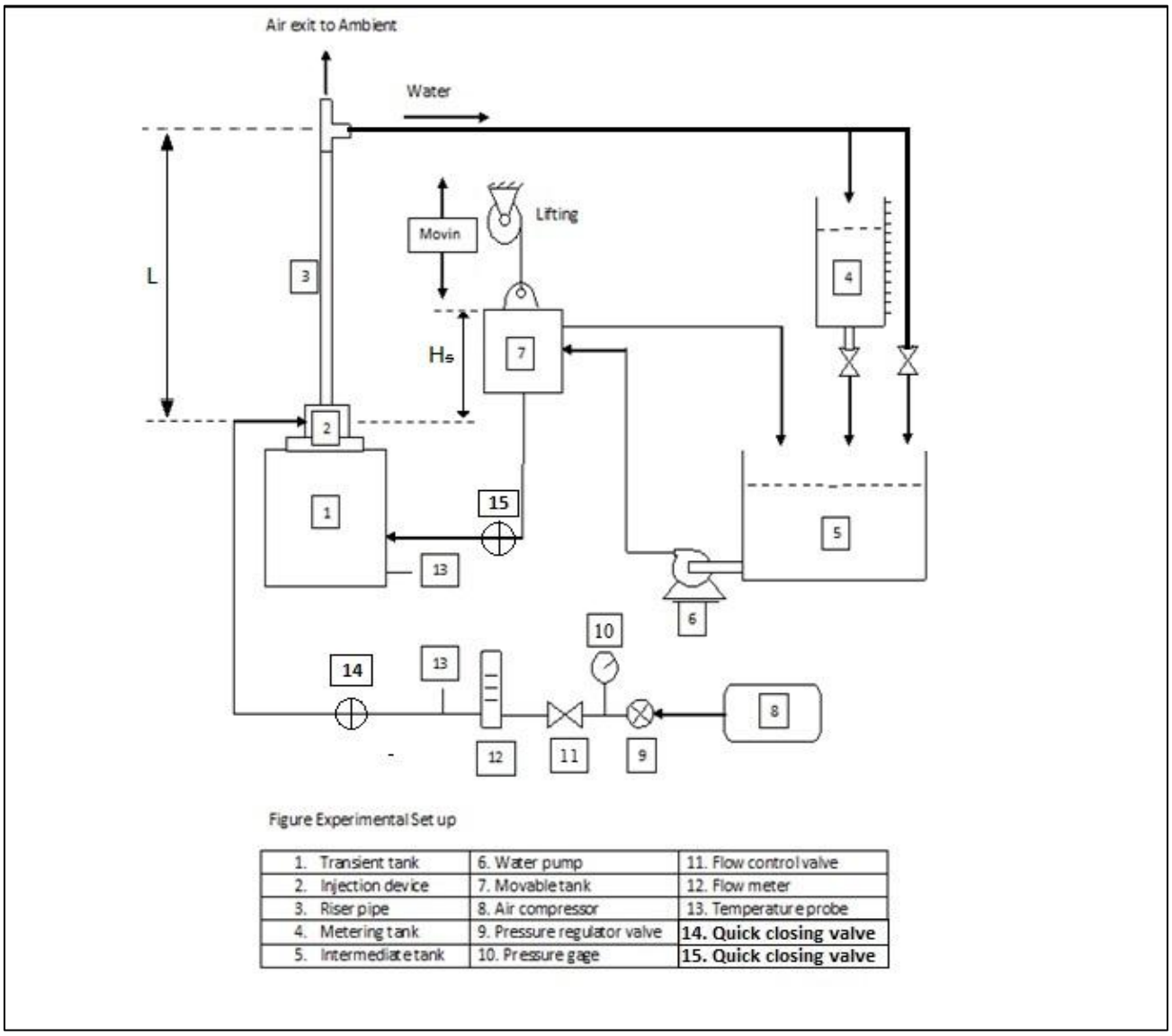

Figure Experimental Set up

1. Transient tank	6. Water pump	11. Flow control valve
2. Injection device	7. Movable tank	12. Flow meter
3. Riser pipe	8. Air compressor	13. Temperature probe
4. Metering tank	9. Pressure regulator valve	**14. Quick closing valve**
5. Intermediate tank	10. Pressure gage	**15. Quick closing valve**

Figure 1. Testing schematics drawing.

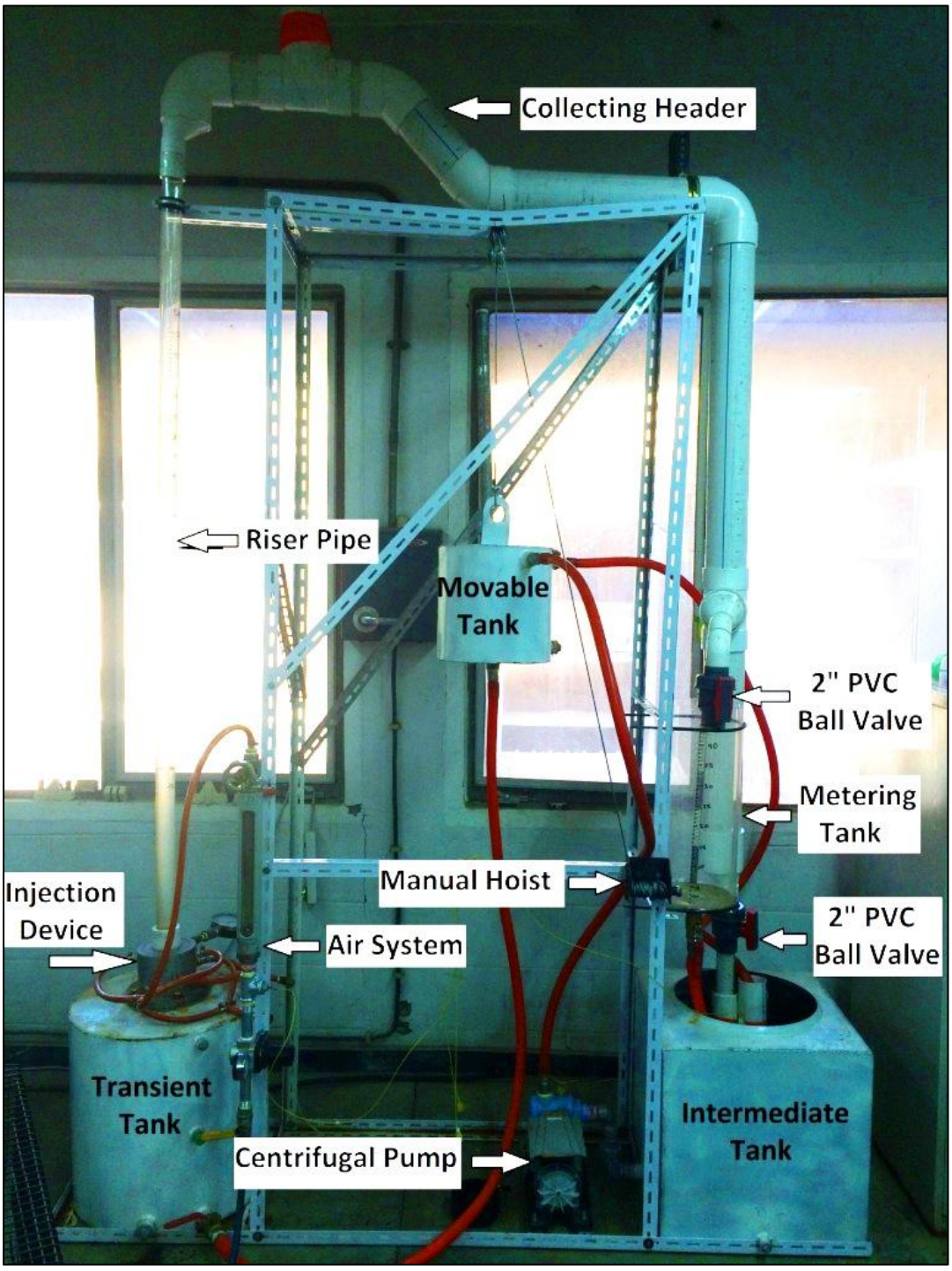

Figure 2. Experimental setup.

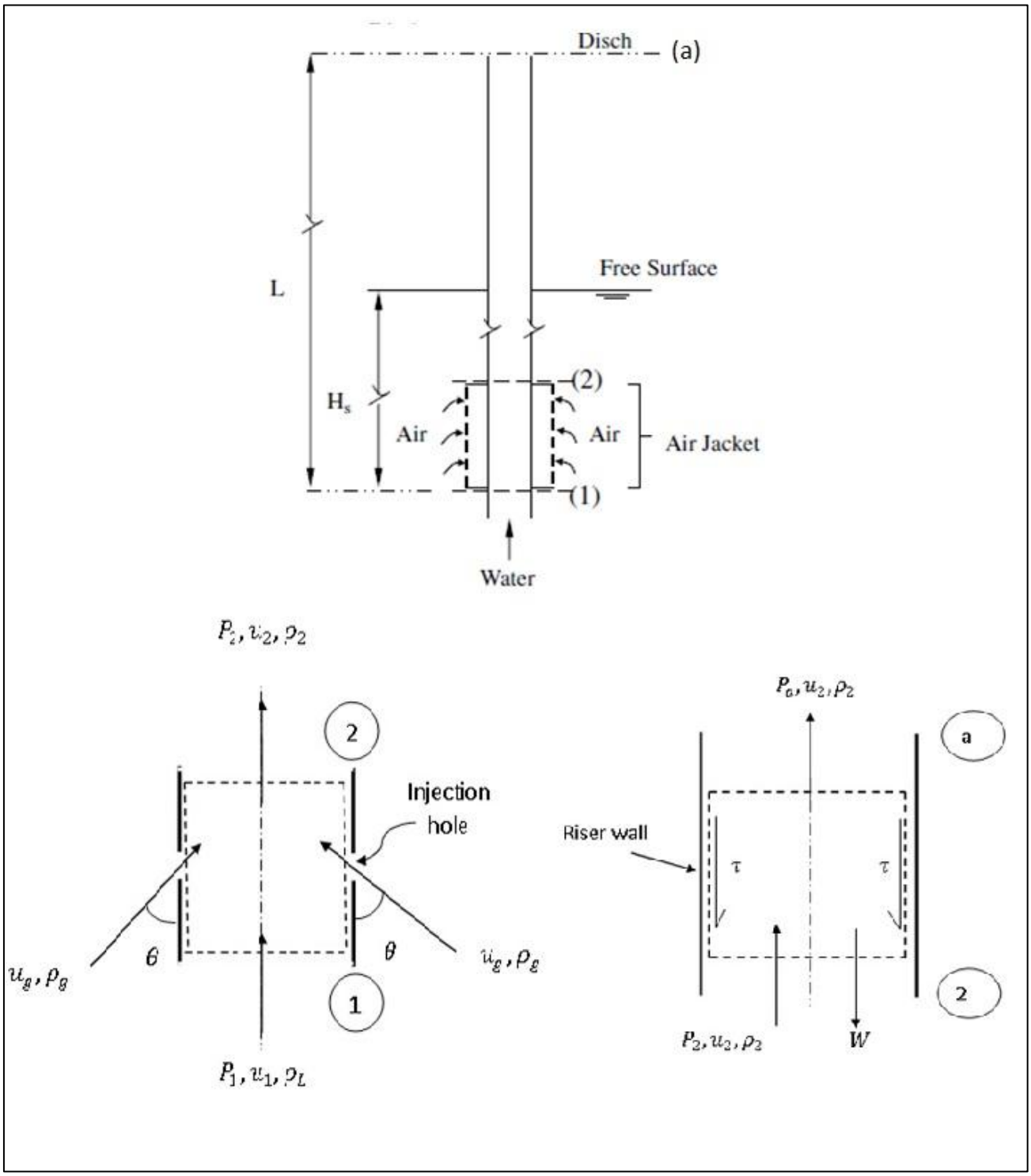

Figure 3. Schematic of airlift pump for analysis.

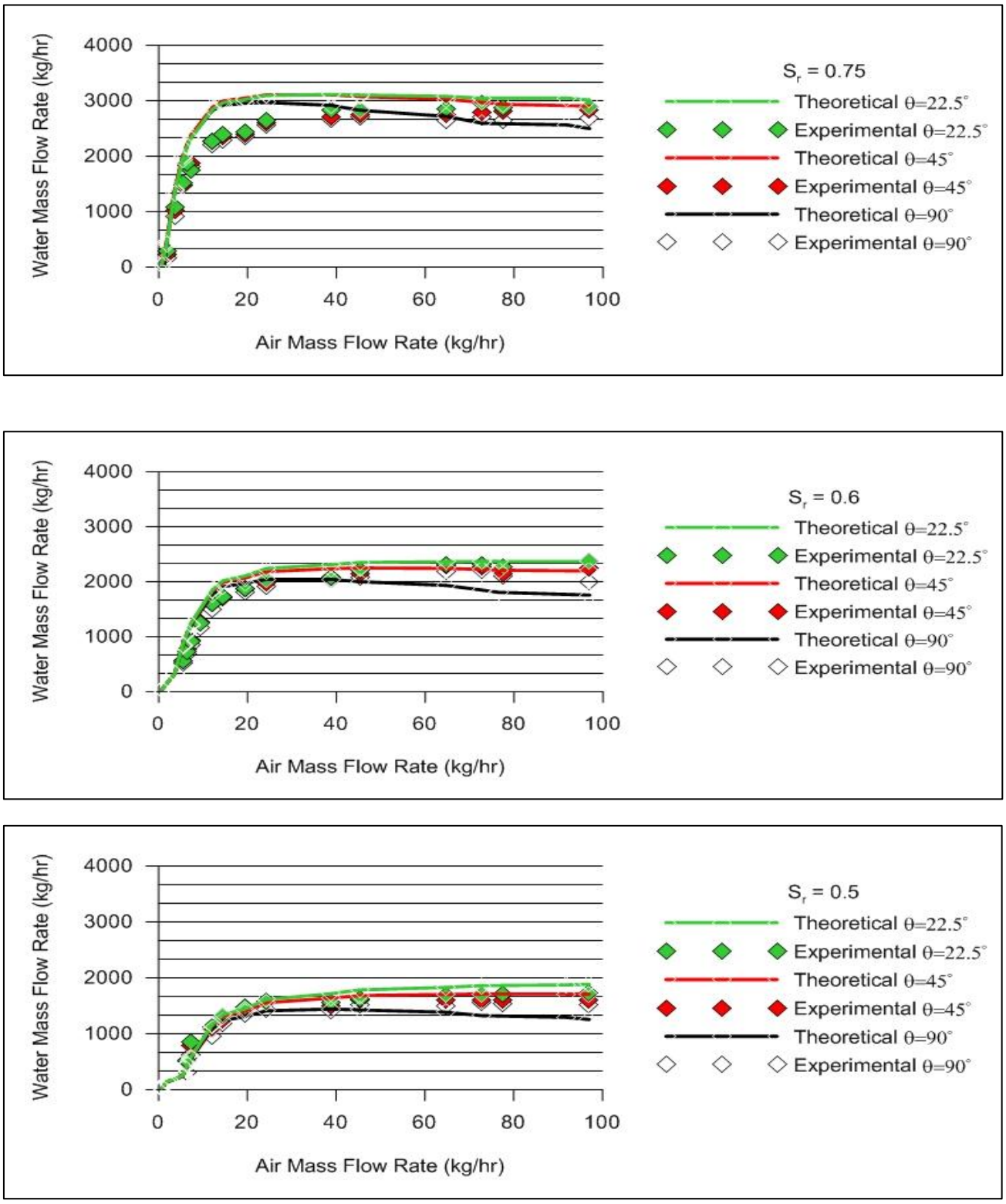

Figure 4. Variation of airlift pump performance curve with various injection angles at submergence ratio (a): 0.75, (b): 0.6 and (c): 0.5.

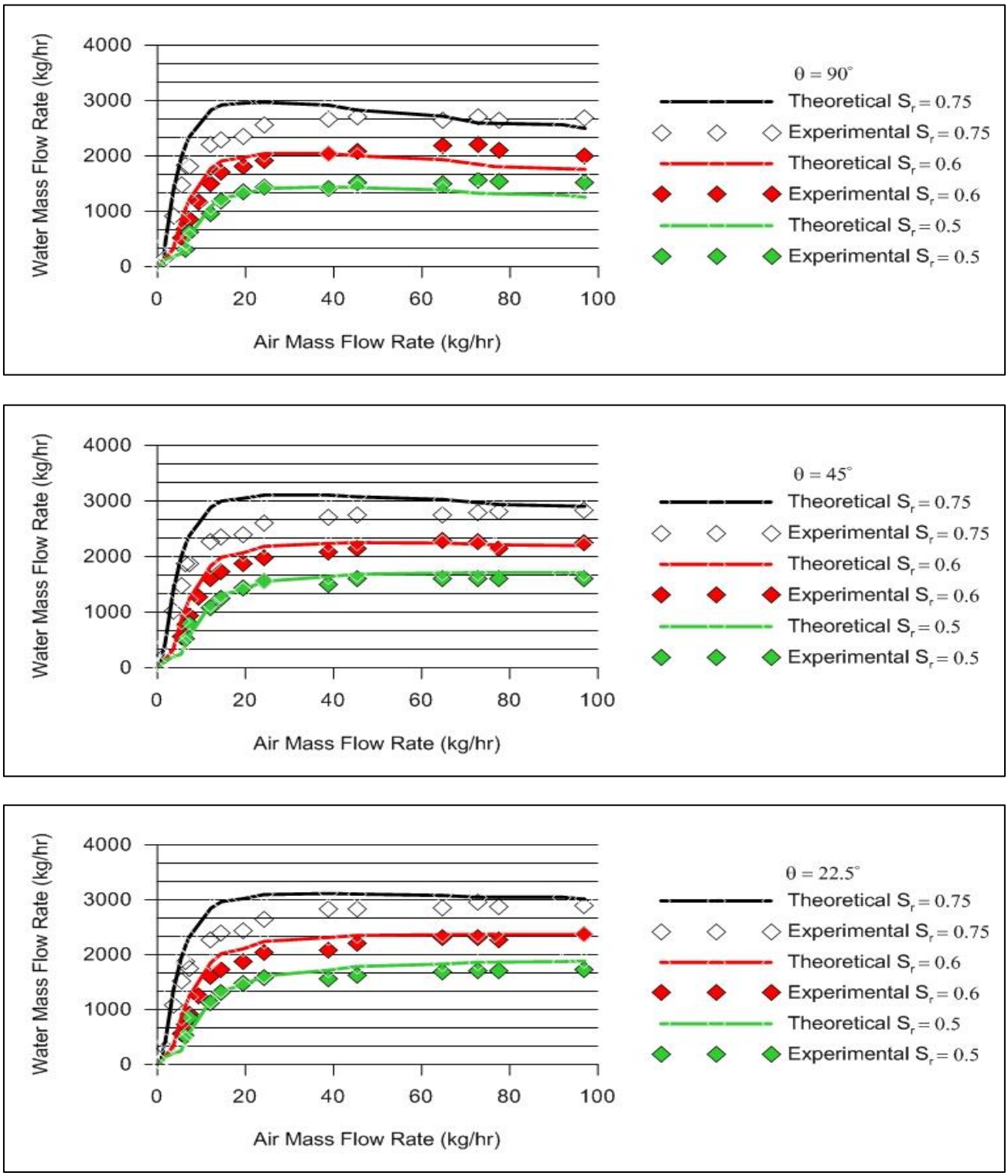

Figure 5. Variation of airlift pump performance curve with various submergence ratio at injection angles (a): 90°, (b): 45° and (c): 22.5°.

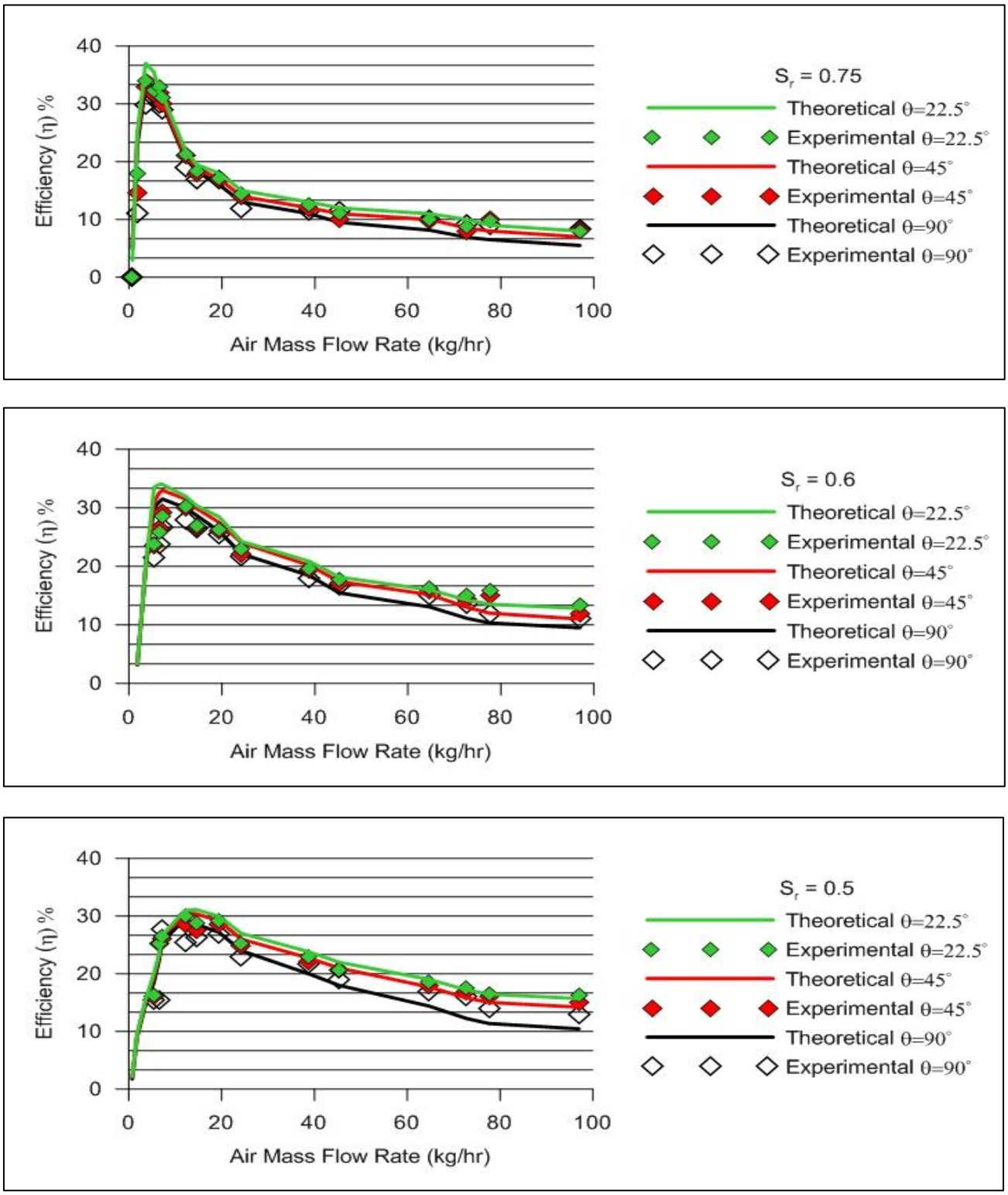

Figure 6. Variation of airlift pump efficiency various submergence ratio at injection angles (a): 90°, (b): 45° and (c): 22.5°.

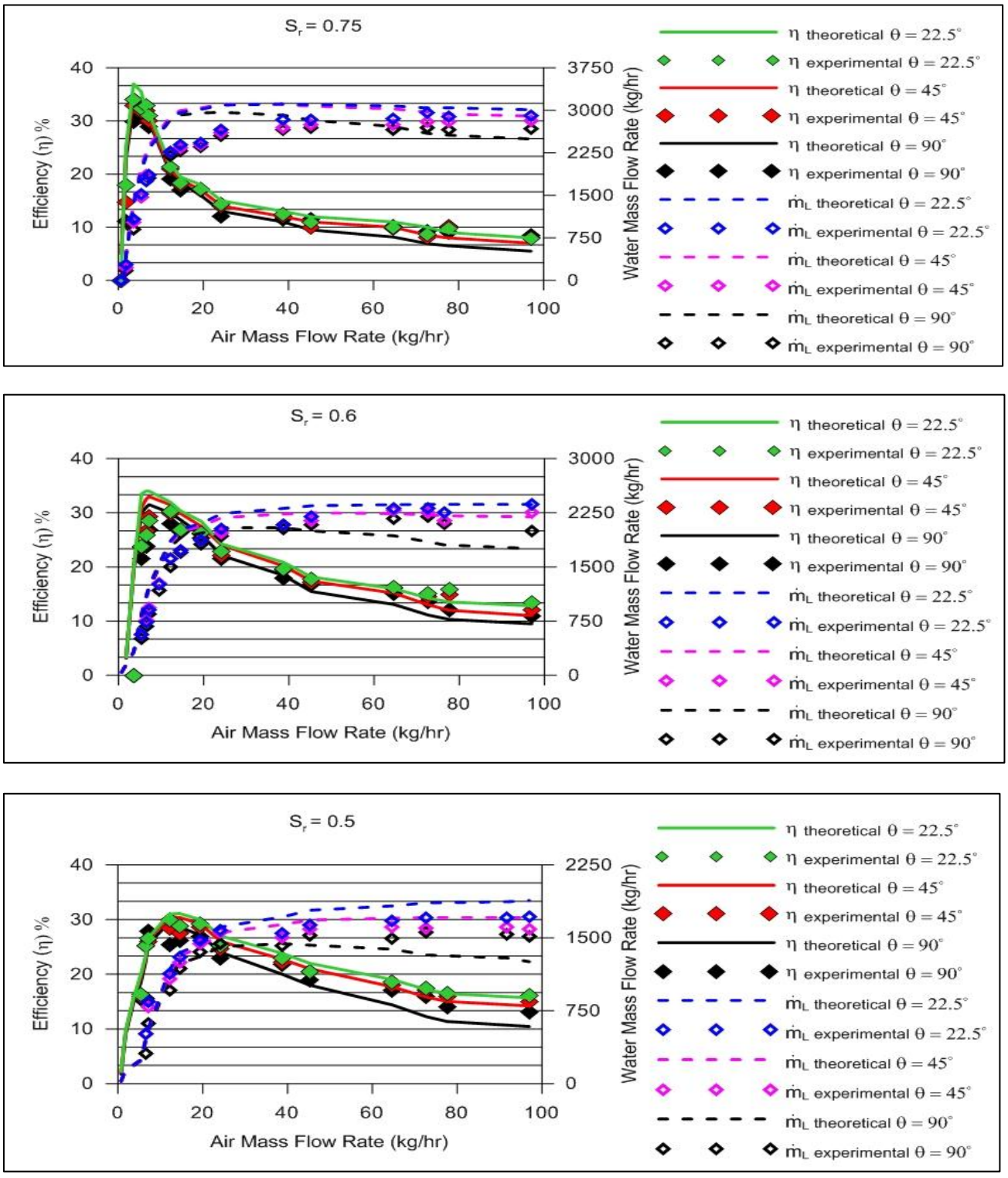

Figure 7. Variation of airlift pump efficiency and performance curve with various submergence ratio at injection angles (a): 90˚, (b): 45˚ and (c): 22.5˚.

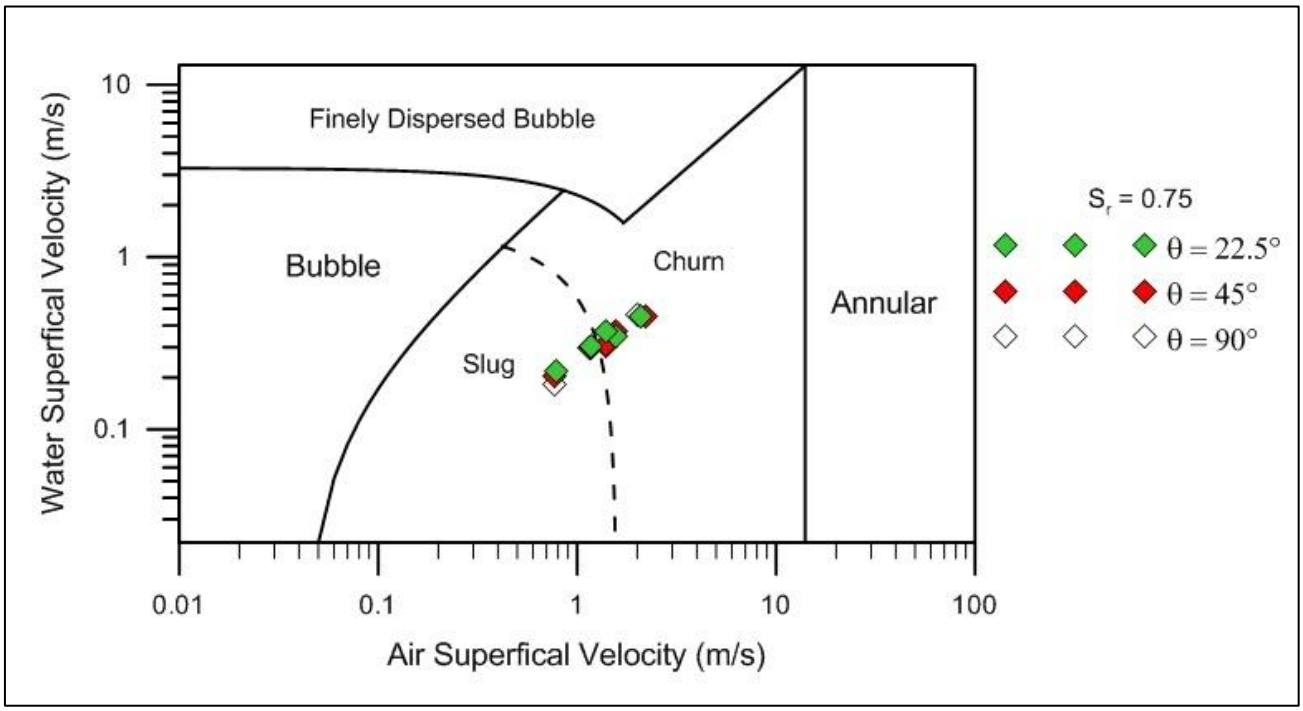

Figure 8. Distribution of experimental best efficiency point for various injection angles on the flow map proposed by, **Taitel et al., 1980**, at submergence ratio (0.75).

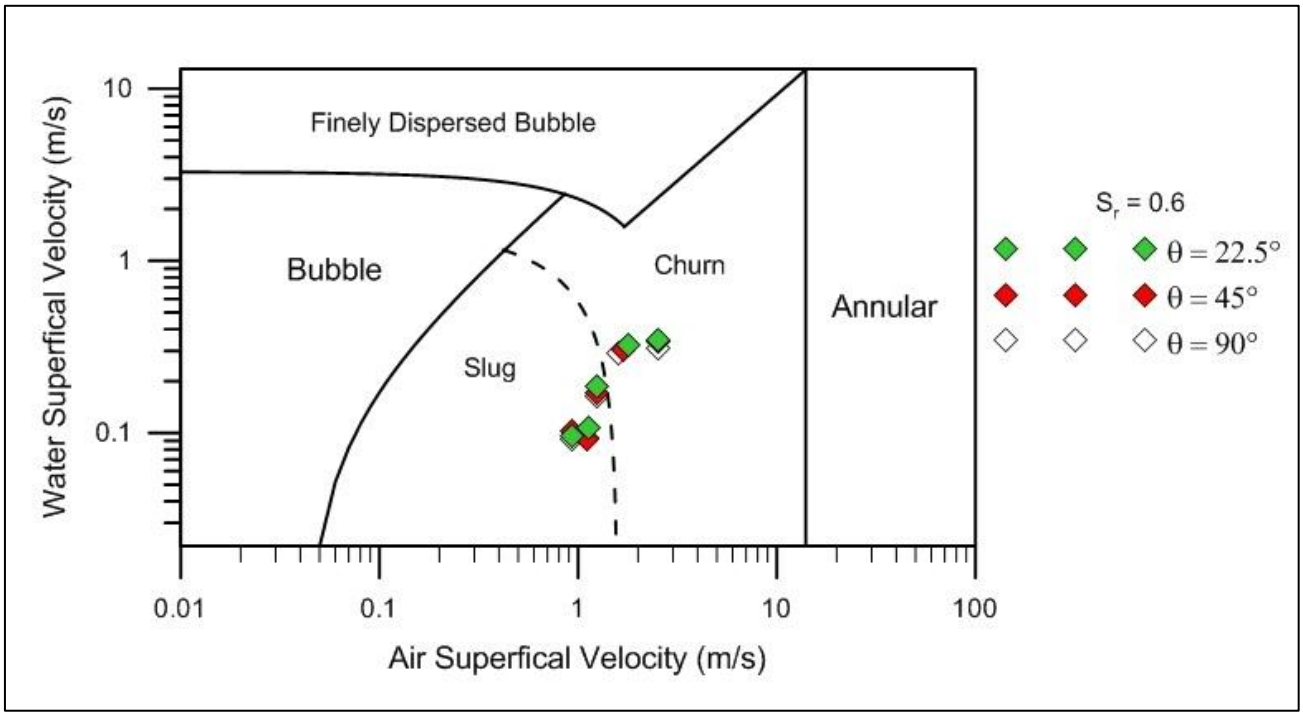

Figure 9. Distribution of experimental best efficiency point for various injection angles on the flow map proposed by, **Taitel et al., 1980**, at submergence ratio (0.6).

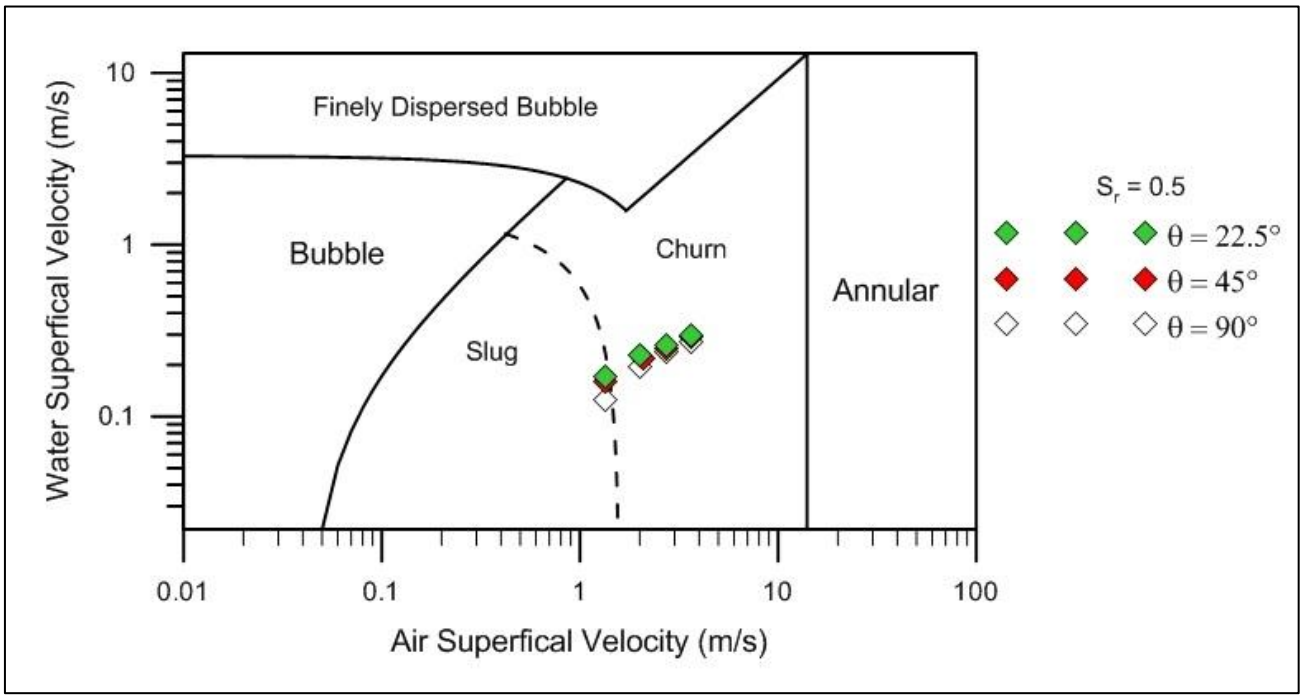

Figure 10. Distribution of experimental best efficiency point for various injection angles on the flow map proposed by, **Taitel et al., 1980**, at submergence ratio (0.5).